WIDEBAND ARRAY IMAGING OF A TARGET SITUATED IN AN UNKNOWN RANDOM MEDIA

Dehong Liu and Lawrence Carin

Department of Electrical and Computer Engineering
Duke University, Durham, NC 27708-0291

ABSTRACT

We propose two new methods for wideband array signal imaging for targets situated in unknown random media. First, a normalized coherent interferometric (N-CINT) imaging algorithm is developed based on coherent interferometric (CINT) imaging theory, yielding improved imaging performance with experimental data. Second, a phase-difference analysis (PDA) method is proposed to significantly reduce computation time and to improve imaging quality. The parameters in the two methods are determined adaptively by optimizing an objective function. Experiments are carried out for electromagnetic scattering using a linear antenna array, providing a demonstration of these methods.

***Index Terms*—** Arrays, random media, imaging

1. INTRODUCTION

Wideband array imaging has been of interest for decades in a wide variety of imaging applications. One of the challenging problems is to image a target situated in an unknown random media. Kirchhoff migration is a widely used approach, assuming that the medium is homogeneous, and it works well in smooth and known media. However, this method is unreliable when applied to data scattered from unknown random inhomogeneous media, since the scattered field may be significantly deformed due to the random inhomogeneous media [1][2]. As an alternative, the time-reversal technique yields super-resolution imaging in random media [3][4], but it requires strict knowledge of the media propagation properties.

Coherent interferometric (CINT) theory was recently proposed in the mathematics community to exploit the coherence of array data in space and frequency [1][2]. In the CINT method, each datum at a given frequency and sensor location is assumed only coherent with its neighbor within a learned spatial and spectral region, which is centered at the given frequency and location and defined by the decoherence frequency and decoherence length. The CINT imaging algorithm adaptively determines the decoherence frequency and length by optimizing a functional [2]. Although simulated results show good performance of the adaptive CINT algorithm in random media when employing a large-aperture array, there are two drawbacks in real applications, based on our experience with data like that considered below. First, the CINT algorithm may fail when there are large variations in the magnitude of the scattering data. Second, the CINT algorithm is computationally time-consuming since the optimization is achieved by searching in a two-dimensional region defined by the decoherence frequency and decoherence length.

To avoid these disadvantages, we first develop a normalized coherent interferometric (N-CINT) algorithm to improve the imaging performance for real applications, by suppressing magnitude variability across the array. The measured data are normalized such that each array element plays an equal role in imaging, which consequently is found to yield improved imaging results on measured data. However, the computational complexity still remains for N-CINT. A phase difference analysis (PDA) method is therefore proposed, which employs the phase difference instead of the two parameters in CINT and N-CINT, to seek a set in which all data points have small phase disturbances and thus are coherent for imaging. This set is obtained adaptively by optimizing the same functional as applied in CINT. The performance of the CINT, N-CINT and PDA algorithms are examined based on data from electromagnetic scattering measurements.

The remainder of the paper is organized as follows. A brief review of the CINT and the N-CINT algorithms is provided in Sec. 2. In Sec. 3 the PDA method is introduced, and the experimental system and example imaging results are presented in Sec. 4. This is followed in Sec. 5 by conclusions.

2. N-CINT ALGORITHM

2.1. CINT theory

Consider an active array, with N linear receivers located at $\mathbf{r}_n, n=1,...,N$, and one transmitter located at $\mathbf{r}_s$, employed to image a target located at unknown position $\mathbf{r}_t$ situated in random media (the media is fixed but unknown, and is assumed to represent one sample from an unknown underlying distribution). The transmitted signal $s(t)$ is a wideband pulse with frequency spectrum $S(\omega)$, and the scattered field produced by the target at receiver $\mathbf{r}_n$ is $P(\mathbf{r}_n, \omega)$. For random media, two intrinsic and characteristic coherence parameters in the array data $P(\mathbf{r}_n, \omega)$ are defined as follows [1][2]: the decoherence frequency Ω_d which is the difference in frequencies ω and ω' over which $P(\mathbf{r}_n, \omega)$ and $P(\mathbf{r}_n, \omega')$ become uncorrelated, and the decoherence length X_d which is the difference in receiver locations $\mathbf{r}_n$ and $\mathbf{r}_{n'}$ over which $P(\mathbf{r}_n, \omega)$ and $P(\mathbf{r}_{n'}, \omega)$ become uncorrelated. The coherent interferometric (CINT) functional is given by[1][2]

$$
\begin{aligned}
&I(\mathbf{r}; \Omega_d, X_d) \\
&= \iint_{|\omega-\omega'|\le\Omega_d} d\omega d\omega' \sum\sum_{|\mathbf{r}_n-\mathbf{r}_{n'}|\le X_d} P(\mathbf{r}_n,\omega)\big(P(\mathbf{r}_{n'},\omega')\big)^* \\
&\exp\{j[\omega(\tau(\mathbf{r}_n,\mathbf{r})+\tau(\mathbf{r},\mathbf{r}_s))-\omega'(\tau(\mathbf{r}_{n'},\mathbf{r})+\tau(\mathbf{r},\mathbf{r}_s))]\}
\end{aligned}
\quad (1)
$$

where $\mathbf{r}$ represents the imaging location and $\tau(\mathbf{r}_a, \mathbf{r}_b)$ is the travel time between location $\mathbf{r}_a$ and $\mathbf{r}_b$. Specifically, (1) is equal to the square of the Kirchhoff migration functional when the array data are coherent over the full frequency band B and the full aperture A, *i. e.*, $\Omega_d = B$, $X_d = A$ [5]. The CINT functional can be viewed as a smoothed version of Kirchhoff migration. Smoothing increases the statistical stability of the image but causes blurring.

For particular random media the coherence parameters are adaptively determined by minimizing the objective function

$$O(\Omega_d, X_d) = \|J(\cdot;\Omega_d, X_d)\|_{L^1(D)} + \|\nabla_{\mathbf{r}} J(\cdot;\Omega_d, X_d)\|_{L^1(D)}, \quad (2)$$

where $J(\mathbf{r};\Omega_d, X_d) = \dfrac{\sqrt{I(\mathbf{r};\Omega_d, X_d)}}{\sup_{\mathbf{r}} \sqrt{I(\mathbf{r};\Omega_d, X_d)}}$ and $L^1(D)$ denotes L^1 norm on imaging domain D. We note that the desired parameters Ω_d and X_d are obtained adaptively by optimizing the functional in (2), which is explicitly based on the quality of the image. This functional penalizes the spurious fluctuations by minimizing the gradient of the image in a norm and controls the blurring by minimizing the image in a sparsity promoting norm; we employ the L^1 norm.

2.2. N-CINT algorithm

To suppress magnitude variability in the array-position-dependent scattering data, we normalize the discrete measured data $P(\mathbf{r}_n, \omega_m)$ by utilizing a complex weight $w_{n,m}$. The normalized data is given as

$$\widetilde{P}(\mathbf{r}_n, \omega_m) = w_{n,m} P(\mathbf{r}_n, \omega_m), \quad (3)$$

where $n = 1,...,N$ and $m = 1,...,M$. The measured data can be decomposed as

$$P(\mathbf{r}_n,\omega_m) = B(\mathbf{r}_n,\omega_m) S(\omega_m) G(\mathbf{r}_t,\mathbf{r}_s,\omega_m) G(\mathbf{r}_n,\mathbf{r}_t,\omega_m), \quad (4)$$

where $G(\mathbf{r}_a,\mathbf{r}_b,\omega_m) = \exp(-j\omega_m\tau(\mathbf{r}_a,\mathbf{r}_b))$ is the Green's function from $\mathbf{r}_a$ to $\mathbf{r}_b$ with the travel time $\tau(\mathbf{r}_a,\mathbf{r}_b)$ in the random media; $B(\mathbf{r}_n,\omega_m)$ is a real coefficient, which includes but is not limited to the effects of the antenna frequency characteristics, and the scattering factor of the target, and the propagation attenuation. We seek to mitigate amplitude variability caused by $B(\mathbf{r}_n, \omega_m)$ and $S(\omega_m)$ by choosing the weight as

$$w_{n,m} = 1/\left[B(\mathbf{r}_n, \omega_m) S(\omega_m)\right]. \quad (5)$$

Substituting (4) and (5) into (3), we obtain

$$\widetilde{P}(\mathbf{r}_n,\omega_m) = G(\mathbf{r}_t,\mathbf{r}_s,\omega_m) G(\mathbf{r}_n,\mathbf{r}_t,\omega_m). \quad (6)$$

For practical implementation, (6) is rewritten as

$$\widetilde{P}(\mathbf{r}_n,\omega_m) = \frac{P(\mathbf{r}_n,\omega_m)}{S(\omega_m)} \left|\frac{S(\omega_m)}{P(\mathbf{r}_n,\omega_m)}\right|. \quad (7)$$

The normalized CINT algorithm is realized by applying the normalized data (7) instead of $P(\mathbf{r}_n, \omega_m)$ into the CINT functional in (1). Similarly, the coherence parameters are adaptively determined by optimizing (2).

3. PDA METHOD

Although the N-CINT algorithm is found in practice to achieve improved imaging results relative to CINT, it is computationally expensive, especially with a large-aperture and wide-bandwidth array. This is because the two coherence parameters are optimized over a large 2D domain, to attain desired imaging quality. Since both parameters are related to the data phase, the phase difference analysis (PDA) method proposed in this paper seeks one parameter, the phase difference, to determine the characteristics of the data coherence. We use normalized data in PDA imaging as applied in the aforementioned N-CINT algorithm (for the same reasons as stated above). For simplicity, the symbol '~' on variables denotes normalized quantities, with normalization implemented as above.

The normalized data in (6) can be expressed as

$$
\begin{aligned}
&\widetilde{P}(\mathbf{r}_n,\omega_m) \\
&= \widetilde{G}_0(\mathbf{r}_n,\mathbf{r}_t,\mathbf{r}_s,\omega_m) + \left[\widetilde{G}(\mathbf{r}_n,\mathbf{r}_t,\mathbf{r}_s,\omega_m) - \widetilde{G}_0(\mathbf{r}_n,\mathbf{r}_t,\mathbf{r}_s,\omega_m)\right]
\end{aligned}, \quad (8)
$$

where $\widetilde{G}(\mathbf{r}_n,\mathbf{r}_t,\mathbf{r}_s,\omega_m)$ is a normalized version of $G(\mathbf{r}_n,\mathbf{r}_t,\mathbf{r}_s,\omega_m) = G(\mathbf{r}_t,\mathbf{r}_s,\omega_m) G(\mathbf{r}_n,\mathbf{r}_t,\omega_m)$ associated with the *random* media from $\mathbf{r}_s$ to $\mathbf{r}_t$ and then back to $\mathbf{r}_n$, while $\widetilde{G}_0(\mathbf{r}_n,\mathbf{r}_t,\mathbf{r}_s,\omega_m)$ represents the same for the corresponding Green's function in a *homogeneous* media, with travel time the same as $\widetilde{G}$. The first term on the right side of (8) yields an ideal image of the target in homogeneous media, while the second term, which represents the disturbance caused by random media, blurs the image. Therefore, in unknown random media, the smaller the disturbance relative to a homogeneous medium, the better the expected imaging quality. The PDA method aims at selecting data points with small phase disturbance for imaging, to improve the overall imaging quality. Since we use normalized data for imaging, only phase information is considered in the PDA method.

Let C denote a set of array data indices (n,m), of which the phase difference between $\widetilde{G}_0(\mathbf{r}_n,\mathbf{r}_t,\mathbf{r}_s,\omega_m)$ and $\widetilde{G}(\mathbf{r}_n,\mathbf{r}_t,\mathbf{r}_s,\omega_m)$ is not greater than a certain value θ_d,

$$C=\left\{(n,m)\middle|\left|Arg\left(\widetilde{G}_0(\mathbf{r}_n,\mathbf{r}_t,\mathbf{r}_s,\omega_m)/\widetilde{G}(\mathbf{r}_n,\mathbf{r}_t,\mathbf{r}_s,\omega_m)\right)\right|\le\theta_d\right\}, \quad (9)$$

where $0\le\theta_d\le\pi$. An image synthesized from C is given as

$$I(\mathbf{r},\theta_d)=\sum_{(n,\,m)\in C}\sum\widetilde{P}^*(\mathbf{r}_n,\omega_m)\exp\left[j\omega_m\left(\tau(\mathbf{r}_n,\mathbf{r})+\tau(\mathbf{r},\mathbf{r}_s)\right)\right]. \quad (10)$$

Since the target position $\mathbf{r}_t$ is unknown, the Green's function $\widetilde{G}_0(\mathbf{r}_n,\mathbf{r}_t,\mathbf{r}_s,\omega_m)$ used to determine C in (9) cannot be computed directly and must be estimated from the measured data. Considering that the phase φ of an electromagnetic wave in homogeneous media is $\varphi=\omega r/c_0$ with the angular frequency ω and the travel distance r, we have $\nabla\varphi=(\nabla\omega\cdot r+\omega\cdot\nabla r)/c_0$, where c_0 is the wave speed. Therefore, the phase of the Green's function $\widetilde{G}_0(\mathbf{r}_n,\mathbf{r}_t,\mathbf{r}_s,\omega_m)$ in homogeneous media can be interpolated approximately by the phases of the four neighbor data points,

$$\begin{aligned}&\varphi_{\widetilde{G}_0}(\mathbf{r}_n,\omega_m)\approx\\&Arg\left(\widetilde{P}(\mathbf{r}_{n-1},\omega_m)+\widetilde{P}(\mathbf{r}_{n+1},\omega_m)+\widetilde{P}(\mathbf{r}_n,\omega_{m-1})+\widetilde{P}(\mathbf{r}_n,\omega_{m+1})\right)\end{aligned}. \quad (11)$$

Substituting (11) into (9), we have

$$C=\left\{(n,m)\middle|\left|Arg\left(\frac{\widetilde{P}_{n-1,\,m}+\widetilde{P}_{n+1,\,m}+\widetilde{P}_{n,\,m-1}+\widetilde{P}_{n,\,m+1}}{\widetilde{P}_{n,\,m}}\right)\right|\le\theta_d\right\}, \quad (12)$$

where a larger θ_d suggests more data points in the set C and less coherence between these data points; θ_d gives a measure of coherence of the data points. Particularly, when $\theta_d=\pi$, all measured data will be used for imaging, and the algorithm reduces to Kirchhoff migration [5]. The parameter θ_d is determined adaptively by minimizing the same objective function as applied in CINT and N-CINT, specifically (2). The PDA method accelerates the optimizing process *vis-à-vis* N-CINT by reducing the optimization space from 2D to 1D, saving significant computation time.

4. EXPERIMENTS

4.1. Experiment setup

The methods outlined in Secs. 2 and 3 are examined based on electromagnetic scattering measurements. For simplicity, a quasi-two-dimensional environment is considered. We constitute a highly scattering random media in a 1.2×1.2 m^2 domain by employing 800 low-loss dielectric rods, as shown in Fig. 1. The rods are of 1.25 cm diameter, 0.6 m length, and with approximate dielectric constant $\varepsilon_r=2.5$. The rods are distributed in a random manner with average inter-rod spacing between rod axes of 6 cm.

A linear *N*-element ($N=13$) sensor array over the 0.5-10.5 GHz band is placed to the left of the random media (see Fig. 1), with inter-element spacing $\Delta=3.0$ cm. The middle (7$^{\text{th}}$) element also works as a transmitter. The elements of the array are identical Vivaldi antennas [6], with the electric fields vertically polarized (electric fields parallel to the rod axes). The antennas are placed at a height that bisects the midpoint of the rods, and the measurements are approximately two-dimensional.

A dielectric target of 0.6 m length, 3.2cm diameter and dielectric constant $\varepsilon_r=2.0$ is placed in the random media. The measurements are performed with a vector network analyzer (HP8720C). Change detection is executed to extract the scattered field of the target. Specifically, it is assumed that scattering data are first obtained in the *absence* of any targets. A second measurement is then performed with the same rod media, but now with the addition of a target. The data with which imaging is performed is based on the difference between these two signals.

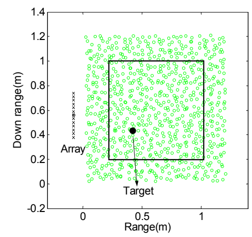

Fig. 1. Top view of measurement setup. The box represents the region for which imaging is performed.

4.2. Experiment results

A dielectric cylindrical target situated in the random media is considered in our experiments. We examine an 80×80 cm^2 imaging domain which covers the target location and this location is randomly picked for general consideration. Fig. 2(a) shows the time domain data measured by the sensor array used in CINT imaging algorithm, and Fig. 2(b) draws the normalized data in N-CINT algorithm as a comparison. We observe that the wavefront of the scattered field in Fig. 2(a) is immersed by clutter but is boosted by normalization in Fig. 2(b), which results in an improved imaging result. The corresponding imaging results using CINT and N-CINT algorithms are presented with 10dB dynamic range in Fig. 3(a) and 3(b) respectively, where the white circle represents the target location and the resolution of the images is 2cm/pixel. The results show that the target is well imaged with N-CINT imaging, but poorly with CINT due to the immersed wavefront as shown in Fig. 2(a). Fig. 4(a) shows the curve of the PDA objective function in (13) with respect to the parameter θ_d, which is roughly convex. We note that a large value of objective function corresponds to either a small θ_d, which results in an over smoothing image, or a large θ_d, which results in an over blurred image. An optimal θ_d is adaptively chosen to minimize the objective function. The corresponding imaging result with this optimal θ_d is shown in Fig. 4(b), where a tight focus at the target position is observed. To perform a quantitative analysis of the imaging quality, a square box is defined corresponding to a contiguous 3×3 pixel (or 6 cm ×6 cm) in the image space. The energy within the box is computed when it is centered over the target (E_c), as well as an average when outside the target region(E_o), and the ratio E_c/E_o is 15.5dB, 12.2dB, and 9.5dB for PDA, N-CINT and CINT, respectively. Furthermore, the corresponding optimal objective function values for the three algorithms are 127.2, 169.3, and 228.1 respectively; and the smaller objective function value indicates better imaging quality. In summary, the PDA yields the best imaging quality among the three algorithms. In addition, the PDA algorithm is computationally more efficient than CINT/N-CINT. It requires roughly 4.5 minutes of CPU in Matlab^{TM} on a Pentium IV PC with 1.73GHz CPU for the PDA algorithm to synthesize a 41×41-pixel image, versus 1 hour for CINT/N-CINT. The performance with noisy data is examined by adding random white Gaussian noise to the measured data. The signal-to-noise ratio (SNR) is computed by normalizing the measured data energy with the variance of the Gaussian noise added. An example result, for which the SNR is 0dB, is shown in Fig. 5(a), (b), and (c) for CINT, N-CINT, and PDA. The image energy ratio defined above at different SNR levels is plotted in Fig. 5(d) for comparison. We note that PDA outperforms N-CINT and CINT at high SNR, but fails at low SNR.

5. CONCLUSIONS

We report two new methods for imaging a target in an unknown random medium using a wideband array. We first develop the normalized coherent interferometric imaging algorithm (N-CINT) by normalizing the measured data to improve imaging performance. Secondly, a phase difference analysis method (PDA) is introduced to exploit the coherence characteristics of real data by measuring phase difference. Both methods yield better imaging performance in practice than CINT when the signal-to-noise ratio is high, while PDA improves the computational speed.

6. REFERENCES

[1] L. Borcea, G. Papanicolaou, and C. Tsogka, "Interferometric array imaging in clutter," *Inv. Prob.*, 21, pp. 1419-1460, 2005.

[2] L. Borcea, G. Papanicolaou, and C. Tsogka, "Adaptive interferometric imaging in clutter and optimal illumination," *Inv. Prob.* 22, pp. 1405-1436, 2006.

[3] G. Lerosey, J. de Rosny, A. Tourin, A. Derode, G. Montaldo and M. Fink, "Time reversal of electromagnetic waves," *Phys. Rev. Letts.*, vol. 92(19), 2004.

[4] P. Blomberg, G. Papanicolaou, and H. K. Zhao, "Super-resolution in time-reversal acoustics," *J. Acoust. Soc. of Amer.*, vol. 111, pp. 230-248, 2002.

[5] N. Bleistein, J. K. Cohen and J. W. Stockwell Jr., *Mathematics of Multidimensional Seismic Imaging, Migration, and Inversion*, Springer, New York, 2001.

[6] Y. Chen, W. T. Joines, Z. Xie, G. Shi, Q. H. Liu, and L. Carin, "Double-sided exponentially tapered GPR antenna and its transmission line feed structure," *IEEE Trans Antenna Propagat.*, vol. 54, no. 9, 2006.

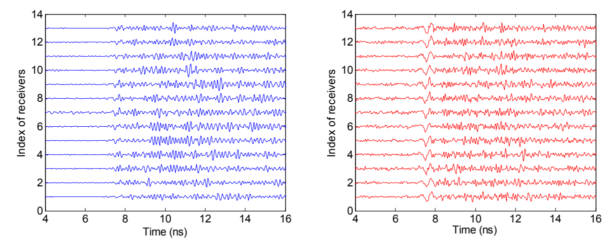

(a) Measured data (b) Normalized data

Fig. 2. Measured array data and normalized array data

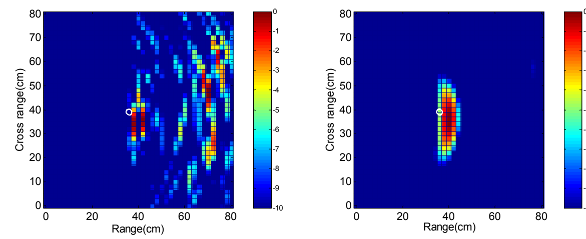

(a) CINT imaging, O=228.1 (b) N-CINT imaging, O=169.3

Fig. 3. Imaging results using data shown in Fig. 2. The minimum of the functional (2) is given for each image.

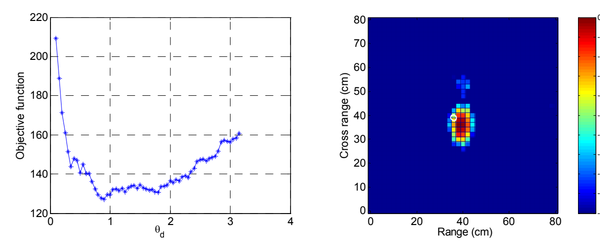

(a) Objective function (b) PDA imaging, O=127.2

Fig. 4. PDA results in adaptive imaging process

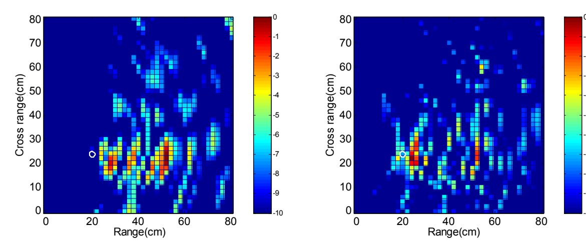

(a) CINT imaging, O=268.88 (b) N-CINT imaging, O=279.2

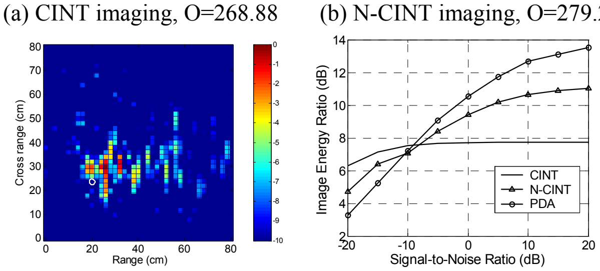

(c) PDA imaging, O=233.0 (d) Performance comparison

Fig. 5. Results with noisy data and performance comparison